

Second order H-PML for anisotropic forward wavefield simulation

Junxiao Li, Kris Innanen and Bing Wang

*li.junxiao@ucalgary.ca

Abstract

The Hybrid perfectly matched layer (H-PML) is extended to simulate second order displacement-stress elastic wave equations. In this report, the simulation results with both H-PML and C-PML in isotropic and anisotropic media are compared. H-PML is capable of absorbing boundary reflections in both isotropic and anisotropic media, but the C-PML only works perfectly in isotropic media. The simulation results with H-PML for both first order and second order elastic wave equations show its efficiency in boundary reflections suppression.

Introduction and Theory

In H-PML, for the new operator $\nabla_{\tilde{x}} = [\frac{\partial}{\partial \tilde{x}}, \frac{\partial}{\partial y}, \frac{\partial}{\partial z}]$, where, $\frac{\partial}{\partial \tilde{x}} = \frac{1}{s_x} \frac{\partial}{\partial x}$, $\frac{\partial}{\partial y} = \frac{1}{s_y} \frac{\partial}{\partial y}$ and $\frac{\partial}{\partial z} = \frac{1}{s_z} \frac{\partial}{\partial z}$. The complex frequency shifted stretched-coordinate metrics s_x , s_y and s_z are

$$s_x = \kappa_x + \frac{d_x + m_{x/z} d_z}{\alpha_x + i\omega} \quad (1)$$

$$s_z = \kappa_z + \frac{m_{z/x} d_x + d_z}{\alpha_z + i\omega},$$

Using the complex coordinate variables \tilde{x} , \tilde{z} to replace the original coordinate variables in elastic wave equations in VTI media, we obtain new displacement-stress equation system in frequency domain

$$-\omega^2 \hat{u}_1 = \frac{1}{\rho} \left(\frac{1}{s_x} \frac{\partial \hat{\sigma}_{11}}{\partial \tilde{x}} + \frac{1}{s_z} \frac{\partial \hat{\sigma}_{13}}{\partial \tilde{z}} \right) \quad (2)$$

$$-\omega^2 \hat{u}_3 = \frac{1}{\rho} \left(\frac{1}{s_x} \frac{\partial \hat{\sigma}_{31}}{\partial \tilde{x}} + \frac{1}{s_z} \frac{\partial \hat{\sigma}_{33}}{\partial \tilde{z}} \right),$$

and

$$\hat{\sigma}_{11} = \frac{1}{s_x} c_{11} \frac{\partial \hat{u}_1}{\partial \tilde{x}} + \frac{1}{s_z} c_{13} \frac{\partial \hat{u}_3}{\partial \tilde{z}} \quad (3)$$

$$\hat{\sigma}_{33} = \frac{1}{s_x} c_{13} \frac{\partial \hat{u}_1}{\partial \tilde{x}} + \frac{1}{s_z} c_{33} \frac{\partial \hat{u}_3}{\partial \tilde{z}},$$

$$\hat{\sigma}_{13} = c_{44} \left(\frac{1}{s_z} \frac{\partial \hat{u}_1}{\partial \tilde{z}} + \frac{1}{s_x} \frac{\partial \hat{u}_3}{\partial \tilde{x}} \right)$$

In order to get the H-PML formulation in time domain, equation set (2) and (3) should be transformed back to time domain by inverse Fourier transform. Take the first equation of equation set (2) as an example, we rewrite it by adding convolutional terms as

$$\frac{\partial^2 u_1}{\partial t^2} = \frac{1}{\rho} \left(DFT^{-1} \left[\frac{1}{s_x} \right] * \frac{\partial \sigma_{11}}{\partial x} + DFT^{-1} \left[\frac{1}{s_z} \right] * \frac{\partial \sigma_{13}}{\partial z} \right) \quad (4)$$

Introducing a new differential operator in the x direction $\partial_{\tilde{x}} = DFT^{-1} \left[\frac{1}{s_x} \right] * \partial_x$, this new operator can further be written as

$$\partial_{\tilde{x}} = \frac{1}{\kappa_x} \partial_x + \psi_x \quad (5)$$

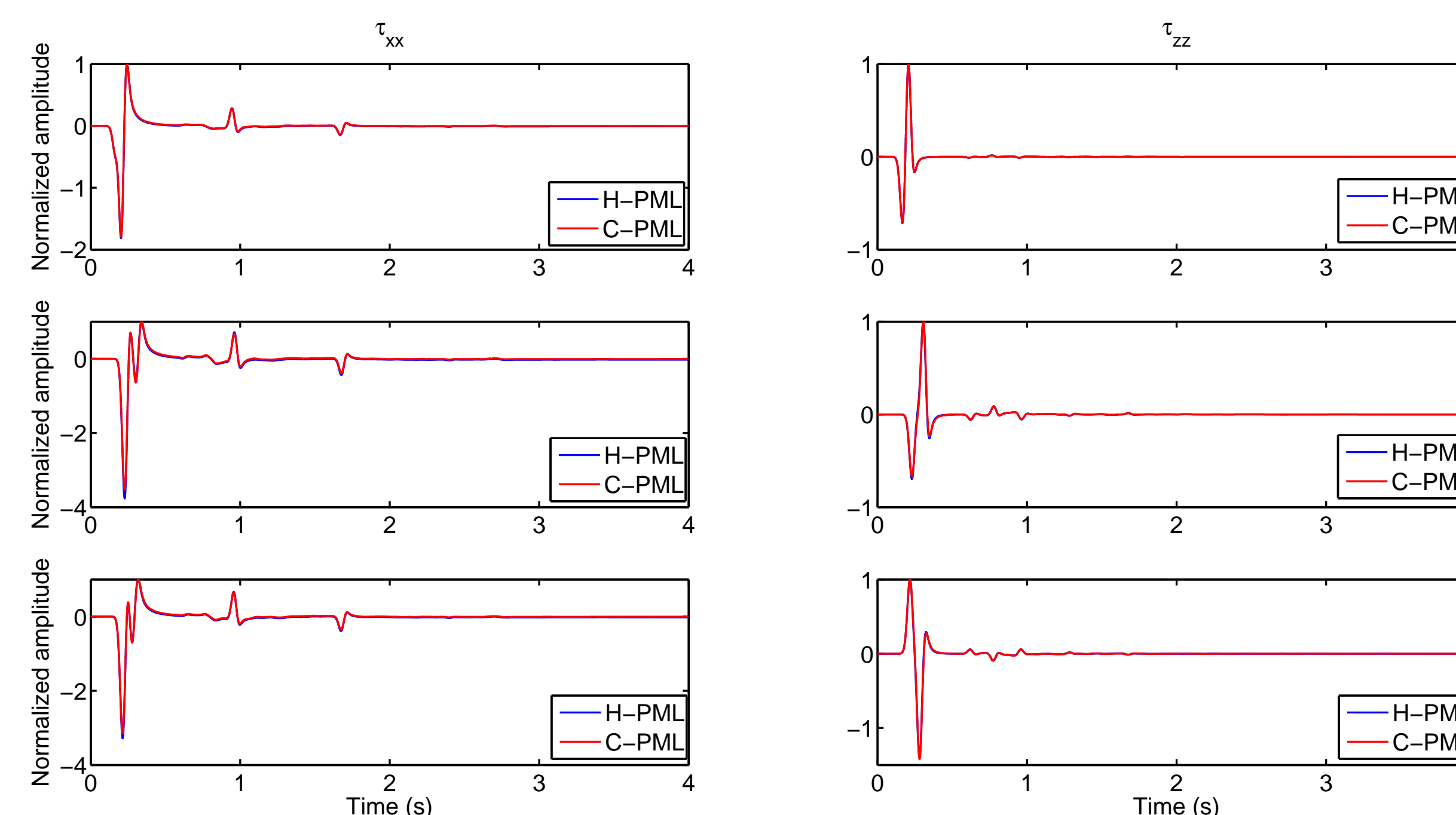
Therefore, equation (4) in time domain can further be expressed as

$$\frac{\partial^2 u_1}{\partial t^2} = \frac{1}{\rho} \left(\frac{1}{\kappa_x} \frac{\partial \sigma_{11}}{\partial x} + \psi_x \sigma_{11} + \frac{1}{\kappa_y} \frac{\partial \sigma_{12}}{\partial y} + \psi_y \sigma_{12} + \frac{1}{\kappa_z} \frac{\partial \sigma_{13}}{\partial z} + \psi_z \sigma_{13} \right) \quad (6)$$

And the first equation of equation set (3) can be rewritten as

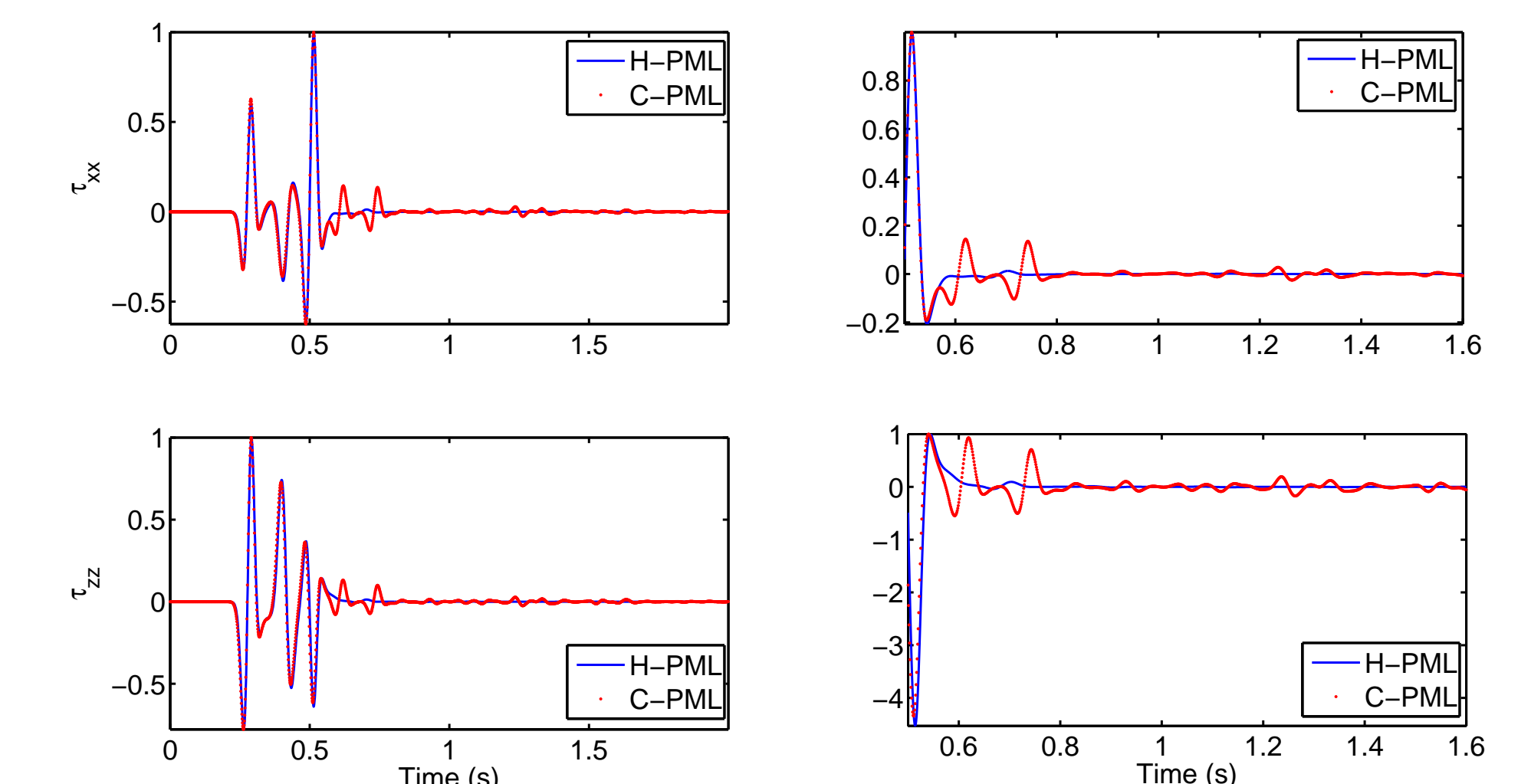
$$\sigma_{11} = c_{11} \left(\frac{1}{\kappa_x} \frac{\partial u_1}{\partial x} + \psi_x u_1 \right) + c_{13} \left(\frac{1}{\kappa_z} \frac{\partial u_3}{\partial z} + \psi_z u_3 \right) \quad (7)$$

Examples

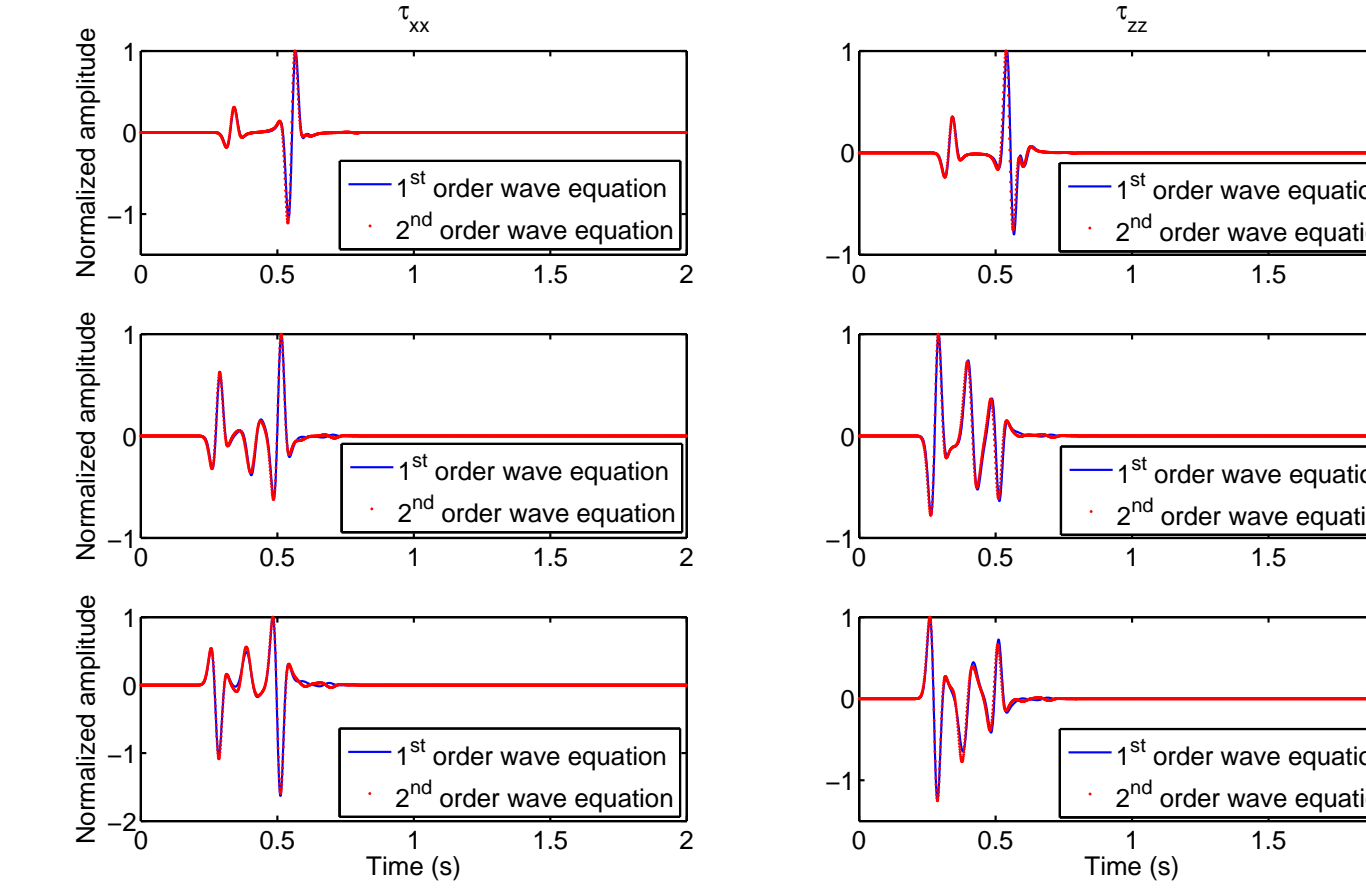
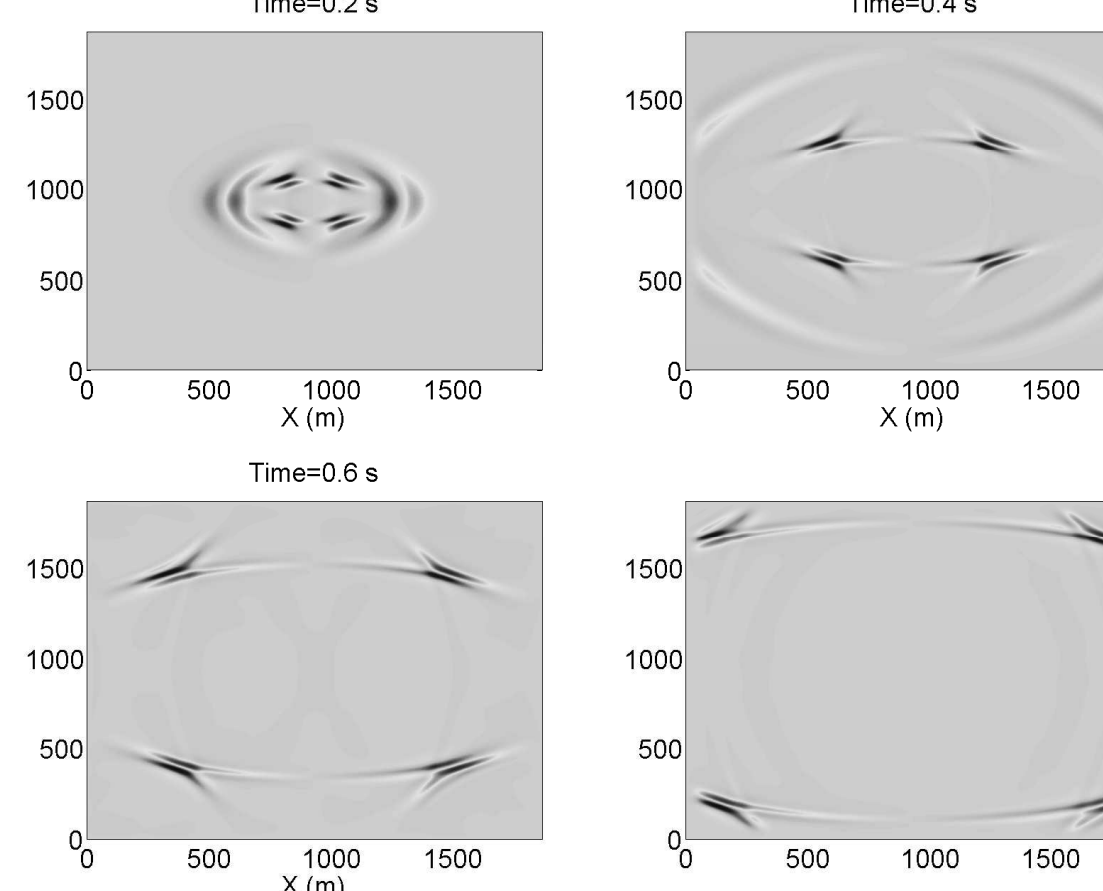


In the above Figure, the time evolutions of the normal stress components τ_{xx} (Left) and τ_{zz} (Right) for three receivers are plotted. In this Figure, simulations with C-PML (red line) matches perfectly with simulations with H-PML (blue line). C-PML and H-PML have almost the same absorbing efficiency for second order displacement-stress wave equations in isotropic media.

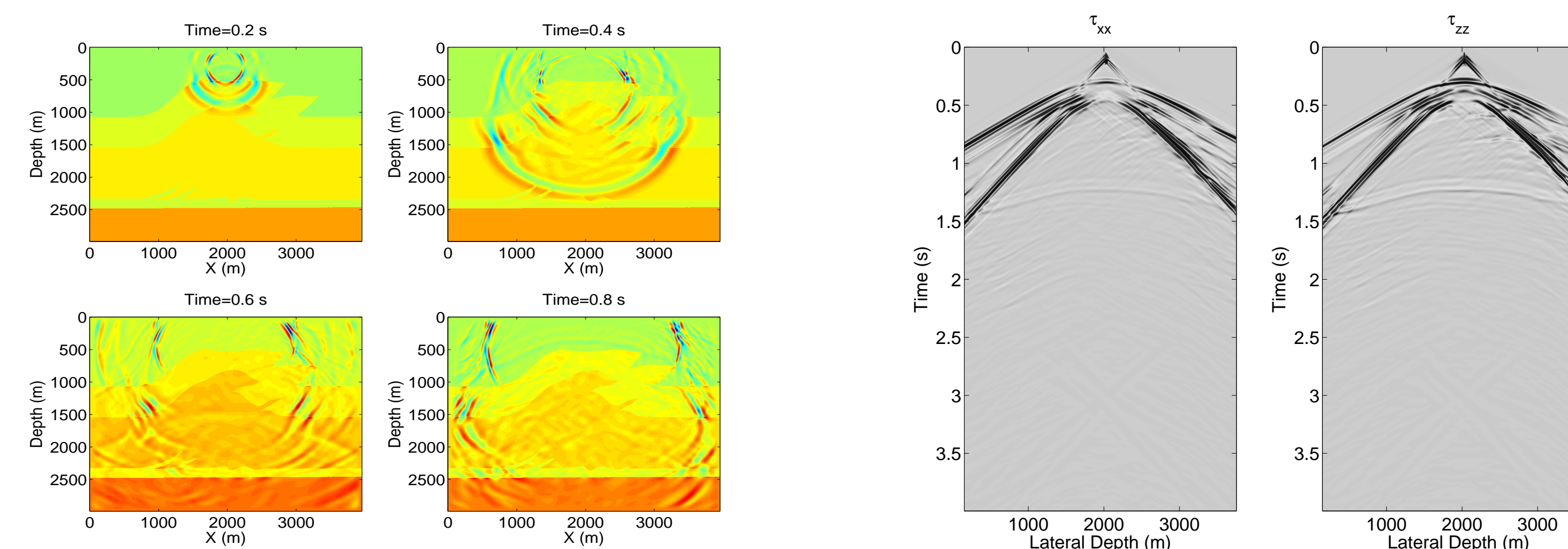
In the Figure below, waveforms of normal stress components in the case of both C-PMLs (red dotted line) and H-PMLs (blue line) for absorbing the boundary wave are displayed. The results demonstrated the efficiency of the H-PML in comparison with the C-PML in this VTI model, especially when we zoom in the results from 0.6 s to 1.6 s, the stress components obtained by using C-PML suffer severely from the oscillations because of the boundary reflections.



In the Right Figure, waveforms of normal stress components in the case of both first order velocity-stress wave equations (blue line) and second order displacement-stress wave equations (red line) with H-PMLs are displayed. For different receivers, the normal stress components both in X direction (Left) and in Z direction (Right) match quite well for the two different wave equation sets. The results demonstrated the efficiency of the H-PML in both the wave equation sets. Snapshots of second-order H-PML is also shown in Left Figure.



Thrust fault model



The next example is the simplified anisotropic thrust fault model, in which anisotropy present through different depth intervals. In Left Figure, a vertical source is located in the upper middle of the fault. With the propagation time increasing, the waveform travels through the model to the boundaries, however, no boundary reflections can be found in each time slice. And the waveforms are absorbed when they travel into the PMLs. In Right figure, the seismograms of stress components σ_{xx} and σ_{zz} show the boundary reflections are effectively suppressed. The receiver stations are evenly spaced along x-direction with a same depth of the source.

Conclusions

In this paper, the H-PML is modified to be applied for suppression of the artificial boundary reflections in second-order wave equations. Its results in both isotropic and anisotropic medium are compared with those of the C-PML approach for the second-order wave equations. The simulation results of the H-PML for first-order and second-order wave equations are also compared. The H-PML can provide satisfying absorbing efficiency for both first and second-order elastic wave equations. And both of the two PMLs are stable and efficient in isotropic medium, yet, instability can be observed in anisotropic medium when C-PML is applied.

Acknowledgement

The authors thank the sponsors of CREWES for continued support. This work was funded by CREWES industrial sponsors and NSERC (Natural Science and Engineering Research Council of Canada) through the grant CRDPJ 461179-13.